

Simulation of Nano Particles in a Laser Trap

Mathias Höld, BSc.

2016

Contents

1	Introduction	3
2	Motivation	5
2.1	Experimental setup	5
2.2	Model of the Surrounding Gas	6
3	Simulation	9
3.1	Molecular Dynamics	9
3.2	The Velocity-Verlet Algorithm	9
3.3	The Nano Particle	13
3.4	The Laser Beam - Energy Influx	15
3.5	The Laser Beam - Trapping	19
3.6	Surrounding Gas - Thermostat	20
4	Results	23
4.1	The Crystal	23
4.2	Velocity Verlet	24
4.3	eHEX	25
4.4	Thermostat	26
4.5	Measurement	26
5	Conclusion and Further Remarks	37

1 Introduction

In the year 1953, Metropolis et al. [1] used the MANIAC (Mathematical Analyzer Numerical Integrator And Computer) at the Los Alamos National Laboratories in the United States to simulate particles in a liquid state to calculate the equation of state. This was the first publication in which scientists used a computer to calculate numerical results based on a physical theory in a process that is to this day called *Metropolis Monte Carlo simulation*. To say that since then a lot has changed in the field of computer simulation (or computers in general) would be a vast understatement.

Not only has the processing power of computers increased exponentially (Moore's law), which allows the simulation of a greater number of particles for a longer period of time, but also new techniques have been developed, such as molecular dynamics, transition path sampling, finite element method etc. These techniques are not only used by physicists, but also find applications in the fields of chemistry, biology, etc., making it possible to apply them to virtually anything. In this thesis we apply methods of simulation to a field of active research: optical trapping. Optical trapping refers to the experimental method of localising small objects with a laser beam. The laser is highly focused on one point, where the object is trapped due to the gradient force of the laser. The size of the trapped objects ranges from a few micrometers down to the subatomic scale.

Optical trapping is a technique that has been used and developed for over 40 years [2]. The idea for this goes back to the beginning of the 20th century, when Lebedev [3], Nichols and Hull [4] demonstrated the existence of a force that light exerts on matter. Due to the technical limitations at that time, the idea was discarded until 1970, where Ashkin [5] used lasers to manipulate the motion of neutral atoms and micrometer sized objects and thus brought the idea of optical trapping back to life.

With this advancement it was possible to develop methods for trapping and manipulating objects of different sizes ranging from the micrometer scale down to the subnano scale. At first, this technique was used to either trap objects in the micrometer range (like cells) or in the subnano scale, where lasers were used for the cooling of atoms. The range between those two, with objects at the scale of one to a hundred nanometer, was not explored as much because neither downscaling the methods for micrometer sized objects nor upscaling the methods for atoms seemed feasible. In recent years however, new developments in the field opened the possibilities to work with a variety of objects in the desired nanometer scale, such as metal nanoparticles [6], nano tubes [7], quantum dots [8] and much more. This non-invasive method of trapping objects allows very precise measurements of various properties and also allows the cooling of nanoparticles towards their quantum mechanical ground state.

1 INTRODUCTION

The small size of the objects used in the optical tweezer experiments make them amenable candidates for computer simulations. In this thesis, I will model an optical tweezer setup, based on a real experiment, to investigate different temperatures in a non-equilibrium state. The experiment features a silica nano sphere trapped in a laser beam within a vacuum chamber. To simulate this experiment, each of these individual parts of the experiment need to be modeled. The silica nano sphere is approximated by a system of argon atoms that interact with each other via a Lennard-Jones potential. These atoms are absorbing energy from the laser and are thus heated up using the enhanced heat exchange algorithm (eHEX) and a harmonic trap is keeping them in place. The gas particles in the gas chamber are acting as a thermostat/barostat and are modeled by a ideal gas pressure bath. In the first chapter, I will introduce two optical tweezer experiments: one conducted by Gieseler et al. to investigate the relaxation of a nano particle from a non-equilibrium steady state and another conducted by Millen et al. to examine different temperature regimes in an optical tweezer experiment. This is followed by the problem statement. The second chapter contains basic information on the techniques used to model the individual parts of the experiment and simulate the dynamic properties. In the third chapter, I will present my findings which are followed by conclusions and further remarks.

2 Motivation

The starting point of this thesis is an experiment conducted by Gieseler et al [9]. It is an optical tweezer experiment, where the motion of a glass nanoparticle in a laser trap was used to investigate the fluctuation theorem[10].

2.1 Experimental setup

In the experiment, a silica nano particle with a radius of about 75 nm and mass of about 3×10^{-18} kg is trapped in a laser beam within a vacuum chamber. The trapping of the silica nano particle is achieved by a gradient force of the laser beam acting on the particle. The experimental setup is depicted in Fig. 1.

The particle fluctuates within the trap in all three spatial directions. These fluctuations are approximately decoupled, which means that they can be described by a one-dimensional Langevin equation:

$$\ddot{x} + \Gamma_0 \dot{x} + \Omega_0^2 x = \frac{1}{m} (F_{\text{fluct}} + F_{\text{ext}}) \quad (1)$$

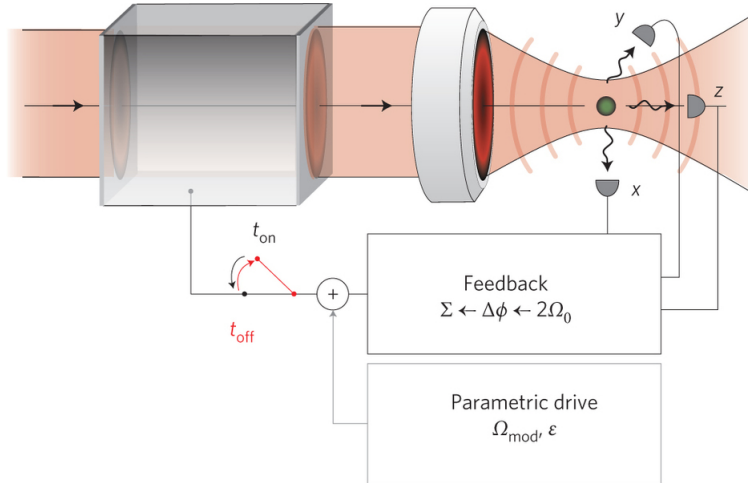


Figure 1: Experimental setup of the optical tweezer experiment. A silica nano particle is trapped in a laser beam via gradient force in a vacuum. The feedback is used to cool down the particle and create a non-equilibrium steady state. In the first part of the experiment, the feedback is turned off and the motion of the particle towards an equilibrated state is observed. In the second part of the experiment, the steady state of the particle is modified by a parametric drive. Both the parametric drive and the feedback are turned off and – as in the first part – the motion of the particle towards an equilibrated state is observed. Figure taken from [9].

On the left hand side of this equation we have the position x of the nano particle (and its derivatives \dot{x} , the velocity and \ddot{x} , the acceleration), the friction coefficient Γ_0 and the angular frequency Ω_0 that describes the fluctuation along

the chosen axis. On the right hand side, there are two forces. The first one is F_{fluct} , which describes a stochastic force caused by interactions with the gas in the vacuum chamber. This force is given by

$$F_{\text{fluct}} = \sqrt{2m\Gamma_0 k_B T_0} \xi(t) \quad (2)$$

where T_0 is the temperature of the heat bath (i.e., the surrounding gas in the vacuum chamber), k_B is the Boltzmann constant and $\xi(t)$ is white noise, which obeys the equations $\langle \xi(t) \rangle = 0$ and $\langle \xi(t)\xi(t') \rangle = \delta(t - t')$, which means that it is a random force. The term Γ_0 appears in the formula (2) due to the fluctuation-dissipation theorem, which links the damping rate to the stochastic force.

The other force, F_{ext} is a time-dependent external force that is applied to the nano particle to create a non-equilibrium steady state. At time $t = t_{\text{off}}$ the force is deactivated and the particle relaxes to a thermally equilibrated state in the laser trap. The evolution of the nano particle from the non equilibrium steady state to the equilibrated state is examined to investigate the fluctuation theorem, which can be written down as

$$\frac{p(-\Delta S)}{\Delta S} = e^{-\Delta S} \quad (3)$$

where ΔS is the relative entropy change given by

$$\Delta S = \beta_0 Q + \Delta\phi \quad (4)$$

In the above equation, Q is the heat absorbed by the bath, β_0 is the reciprocal temperature at which the heat is absorbed and $\Delta\phi$ is the difference of the trajectory dependent entropy. The fluctuation theorem [11], as expressed in (3), states that there is a measurable probability for a finite system to violate the second law of thermodynamics for finite times. This does not stand in contradiction to the second law of thermodynamics itself, as it applies only to short times and does not happen for large systems or long time scales.

The investigation of the fluctuation theorem is performed for two different external forces. The first one is a feedback force and the second one is the feedback force combined with a parametric drive. The results show that the relaxation process for both initial non-equilibrium steady states generated by the external forces demonstrates the validity of the fluctuation theorem.

2.2 Model of the Surrounding Gas

J. Millen et al. [12] worked on a similar experimental setup (without the feedback mechanism) and investigated the heating of the particle in the trap as well as the gas surrounding the particle.

They start from the premise that there are 4 different temperatures one has to consider in such an experiment: the temperature of the gas particles before interacting with the nano particle T_{imp} (for *impinging*), the temperature of the gas particles after interaction T_{em} (for *emerging*), the *surface* temperature of the nano particle T_{sur} and the temperature of the *center of mass* of the nano particle T_{COM} . The experimental setup and the different temperatures are shown in Fig. 2.

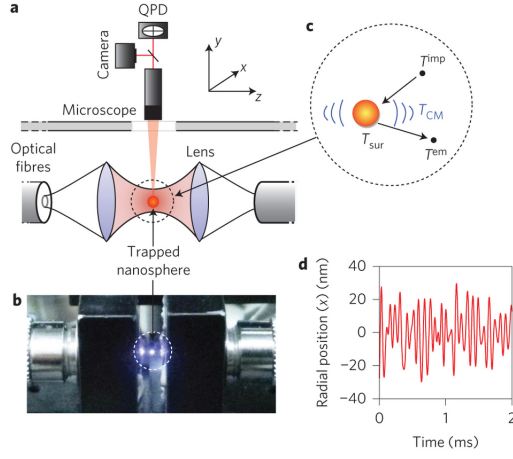


Figure 2: The experimental setup used by Millen et al. In **a** the experiment is schematically depicted and **b** shows a photograph of the actual experimental setup. In **c** the 4 different temperatures that are present during the experiment are illustrated and **d** shows the position of the particle in the trap over time. The image was taken from [12].

The nano particle in the trap is absorbing heat from the laser which causes the surface temperature of the nano particle to be higher than the temperature of the surrounding gas. The impinging gas particles interact with the sphere, absorb some of the energy and emerge with a different temperature, which is in general not equal to the surface temperature. This means that the two temperatures of the gas, T_{imp} and T_{em} , are not equal, the gas surrounding the nano particle is not in a thermal equilibrium, which is in contrast to the assumptions made in many optical tweezer experiments. Since the gas particles only interact with the nano particle in the trap and not which each other, this situation creates two heat baths of different temperatures with the nano particle acting as a mediator between those two baths. This situation is depicted in Fig. 3.

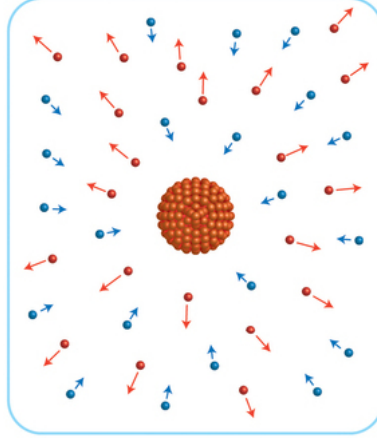


Figure 3: Schematic picture of the two heat baths. The (hot) nano particle interacts with the (cold) incoming gas particles and they leave with a higher temperature. The incoming and outgoing particles do not interact with each other and thus create two separate heat baths with different temperatures. Image modified from [13].

The one dimensional Langevin equation (1) has to be modified to include the different friction coefficients of the two heat baths. The model derived in [12] is described in the following equation:

$$M\ddot{x}(t) + M(\Gamma^{\text{imp}} + \Gamma^{\text{em}})\dot{x}(t) + M\omega^2x(t) = F^{\text{imp}} + F^{\text{em}} \quad (5)$$

where x is the position of the nano particle, \dot{x} and \ddot{x} are the velocity and the acceleration, respectively, M is the mass, ω is the trap frequency, Γ^{imp} and Γ^{em} are the damping constants for the impinging particles and the emerging particles, respectively and F^{imp} and F^{em} are the associated noise terms, which satisfy $\langle F^{\text{imp}} \rangle = \langle F^{\text{em}} \rangle = 0$ individually.

Miller et al. investigate the dependence of the emerging temperature T_{em} on the intensity of the laser for different sized nano particles and different pressures.

With these four temperatures introduced, some questions arise about the relationship between these temperatures. For this theses, I want to focus on the question: how does the laser intensity influence the motion of the nano particle in the laser trap and its center of mass velocity?

In the next section I will introduce the methods that will be used to simulate the system, followed by the results of the simulations and the conclusion of this thesis.

3 Simulation

The problem at hand can be studied on an atomic level with the use of computer simulation. There is a variety of methods for computer simulations that are widely used, one of which being molecular dynamics (MD) simulations.

The goal is to simulate the experiment depicted in Fig. 1 as accurately as possible. To achieve this, the setup has to be broken down into individual pieces that can be modeled by using existing methods. The nano particle will be approximated by a cube of particles, located on the sites of a FCC (face-centered cubic) lattice that interact via a Lennard-Jones potential. The laser serves two purposes: heating up and trapping the particle. The nano particle will be heated up using the eHEX algorithm and trapped using a harmonic potential. Surrounding the nano particle will be a gas chamber, that acts as a thermostat in the simulation, which will be modeled as a cubic box surrounding the nano particle. This box is filled with gas particles that interact with the nano particle via a soft-sphere potential and do not interact with one another.

The following section will give a brief overview of the concepts used to simulate every part of the experiment.

3.1 Molecular Dynamics

Molecular dynamics [14] simulations is a technique for simulating, as the name suggests, the dynamics of a classical many-body system. In this case, classical means, that the trajectories of the individual particles are calculated using classical mechanics rather than quantum mechanics. For relatively big atoms/molecules this is a very good approximation, whereas for systems consisting of hydrogen or helium the effects of quantum mechanics cannot be neglected and other methods have to be used.

The dynamics of the system are obtained by solving Newton's equations of motion for every particle.

3.2 The Velocity-Verlet Algorithm

When we look at the system from a microscopic standpoint, we see that it follows some kind of path in the phase space as time progresses. Every point in this space corresponds to a set of positions and momenta and the connection between two points corresponds to the evolution of the system from one state to another. As mentioned above, this evolution (the dynamics of the system) is a crucial element to molecular dynamics. Since the equations of motion cannot be solved analytically in general, we need to approximate the solution.

The method used here is called finite difference approach. The trajectory of the

system in the phase space is cut into finite pieces of length Δt and the equations of motion are solved for every segment separately (see Fig. 4).

There are several ways to solve this kind of problem, but since we are interested in implementing it into a computer program the ideal solution should have some basic properties [15]:

- It should be fast and require little memory
- It should permit the use of a large time step Δt
- It should duplicate the classical trajectory as closely as possible
- It should satisfy known conservation laws
- It should be simple and easy to program

One algorithm that has all of the above mentioned features is the one proposed by Verlet [16]. In his paper, Verlet starts by Taylor expanding the coordinate vector \mathbf{r}_i for one particle after one time step Δt :

$$\mathbf{r}_i(t + \Delta t) = \mathbf{r}_i(t) + \dot{\mathbf{r}}_i(t)\Delta t + \frac{1}{2}\ddot{\mathbf{r}}_i(t)\Delta t^2 + \frac{1}{3!}\dddot{\mathbf{r}}_i(t)\Delta t^3 + \mathcal{O}(\Delta t^4) \quad (6)$$

Since the first derivative of the coordinate is the velocity, $\dot{\mathbf{r}}_i(t) = \mathbf{v}_i(t)$, and the second derivative of the coordinate is the acceleration, $\ddot{\mathbf{r}}_i(t) = \mathbf{a}_i(t)$, using Newton's law $\mathbf{F}_i(t) = m_i \mathbf{a}_i(t)$ equation (6) can be written as:

$$\mathbf{r}_i(t + \Delta t) = \mathbf{r}_i(t) + \mathbf{v}_i(t)\Delta t + \frac{1}{2m}\mathbf{F}_i(t)\Delta t^2 + \frac{1}{3!}\ddot{\mathbf{r}}_i(t)\Delta t^3 + \mathcal{O}(\Delta t^4) \quad (7)$$

The same calculation can be carried out for one time step before t :

$$\mathbf{r}_i(t - \Delta t) = \mathbf{r}_i(t) - \mathbf{v}_i(t)\Delta t + \frac{1}{2m}\mathbf{F}_i(t)\Delta t^2 - \frac{1}{3!}\ddot{\mathbf{r}}_i(t)\Delta t^3 + \mathcal{O}(\Delta t^4) \quad (8)$$

The sum of these two equations yields

$$\mathbf{r}_i(t + \Delta t) + \mathbf{r}_i(t - \Delta t) = 2\mathbf{r}_i(t) + \frac{1}{2}\mathbf{F}_i(t)\Delta t^2 + \mathcal{O}(\Delta t^4) \quad (9)$$

and from this we get the final form for the new coordinates:

$$\mathbf{r}_i(t + \Delta t) = 2\mathbf{r}_i(t) + \mathbf{r}_i(t - \Delta t) + \frac{1}{2}\mathbf{F}_i(t)\Delta t^2 \quad (10)$$

This means that the new coordinates can be calculated using the current coordinates, the current forces and the coordinates from the past time step.

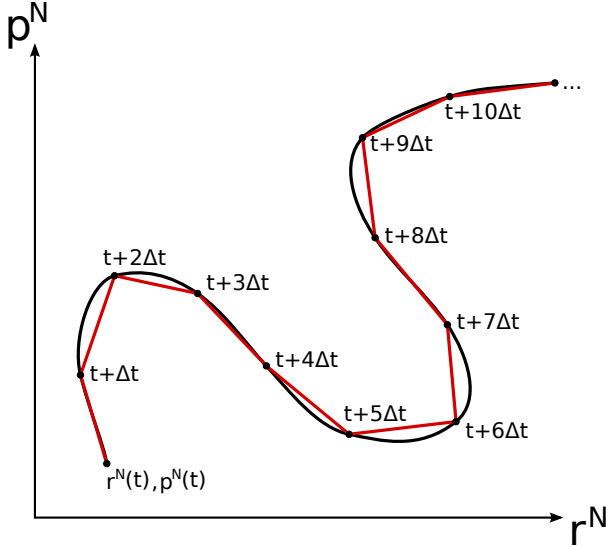


Figure 4: Simplified graphical schematic of the finite difference approach. The evolution of the system from a point $(r^N(t), p^N(t))$ in the phase space is approximated by slicing it up into pieces of length Δt . On every stop after the starting point ($t + \Delta t, t + 2\Delta t, t + 3\Delta t, \dots$) the equations of motion can be solved numerically.

From equation (10) one thing becomes clear: the velocities are not necessary to calculate the new positions and they are not computed in the process, but for the calculation of i.e. the kinetic energy the velocities are needed. Thus, the velocities have to be calculated with a combination of the Taylor expansions of the coordinate vectors at $t + \Delta t$ and $t - \Delta t$:

$$\mathbf{r}_i(t + \Delta t) - \mathbf{r}_i(t - \Delta t) = 2\mathbf{v}_i(t)\Delta t + \mathcal{O}(\Delta t^3) \quad (11)$$

which can be rewritten as

$$\mathbf{v}_i(t) = \frac{\mathbf{r}_i(t + \Delta t) - \mathbf{r}_i(t - \Delta t)}{2\Delta t} + \mathcal{O}(\Delta t^2) \quad (12)$$

This approach has the advantage that it is fast, requires little memory and is reliable in the sense that there is no energy drift occurring during the simulation, which means that the energy is conserved. When we compare this to the list of desired properties this seems like a good algorithm.

This algorithm however has two significant disadvantages. The first one is the calculation of the velocities. As can be seen in equation (12), the accuracy of the calculation is only $\mathcal{O}(\Delta t^2)$ while the positions can be calculated with an error of order Δt^4 . The other big disadvantage is the first step of the algorithm. Since the calculation of the new positions requires the current positions and the ones from one time step before, which technically do not exist.

The solutions to this problem is to include the stepwise calculation of the velocities [17]. For this we start again with the Taylor expansion of the coordinates vector (7) and instead of Taylor expanding $\mathbf{r}_i(t - \Delta t)$, we write it as

$$\mathbf{r}_i(t) = \mathbf{r}_i(t + \Delta t) - \mathbf{v}_i(t + \Delta t)\Delta t + \frac{1}{2m}\mathbf{F}_i(t + \Delta t)\Delta t^2 \quad (13)$$

Using (7) in the abvove equation we get

$$\begin{aligned} \mathbf{r}_i(t) &= \mathbf{r}_i(t) + \mathbf{v}_i(t)\Delta t + \frac{1}{2m}\mathbf{F}_i(t)\Delta t^2 \\ &\quad - \mathbf{v}_i(t + \Delta t)\Delta t + \frac{1}{2m}\mathbf{F}_i(t + \Delta t)\Delta t^2 \end{aligned} \quad (14)$$

and thus

$$\mathbf{v}_i(t + \Delta t) = \mathbf{v}_i(t) + \frac{1}{2m}(\mathbf{F}_i(t) + \mathbf{F}_i(t + \Delta t))\Delta t \quad (15)$$

With the addition of this equation this algorithm is called the Velocity-Verlet algorithm, which is summarized in the following two equations:

$$\begin{aligned} \mathbf{r}_i(t + \Delta t) &= \mathbf{r}_i(t) + \mathbf{v}_i(t)\Delta t + \frac{1}{2m}\mathbf{F}_i(t)\Delta t^2 \\ \mathbf{v}_i(t + \Delta t) &= \mathbf{v}_i(t) + \frac{1}{2m}[\mathbf{F}_i(t) + \mathbf{F}_i(t + \Delta t)]\Delta t \end{aligned} \quad (16)$$

This algorithm is self starting, uses a small amount of memory, conserves the energy (not exactly) and gives a very good approximation to the originial trajectory in the phase space. To program this algorithm the following steps are needed:

1. Calculate all the forces between the particles (for the first step only)
2. Calculate the new positions with current velocity and forces
3. Calculate first half of the new velocities with current forces
4. Calculate all the forces for the new position
5. Use new forces to calculate second half of new velocities

The first point only has to be carried out for the first step, because the forces have not been calculated at this point. As the forces are calculated for the new positions in step 4, they can be used for the next time step. For the first time step the velocities have to be chosen randomly and are calculated with this algorithm from that point forward.

3.3 The Nano Particle

The glass particle from the experiment will be modeled as a system of particles interacting via a Lennard-Jones pair potential,

$$U(r) = 4\epsilon \left[\left(\frac{\sigma}{r} \right)^{12} - \left(\frac{\sigma}{r} \right)^6 \right] \quad (17)$$

where ϵ is the depth of the potential well (and thus its unit is energy) and σ is the distance at which the potential is zero. The form of the potential and the relation to the parameters is depicted in Fig. 5. Since ϵ and σ are crucial parameters for

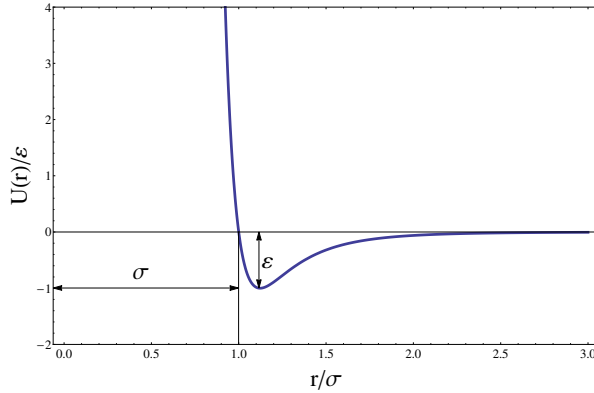


Figure 5: The Lennard-Jones 12-6 potential from (17). The x-axis is the particle distance divided by σ and the y-axis is the potential divided by the depth of the potential well.

the simulation and do not change over time, it is practical to use them to define the dimensions of the system. This means that the unit of distance is σ , the unit of energy is ϵ and the unit of mass is the mass of the simulated particle. The so called *reduced units* can be constructed from these three parameters and put into relation to the original units. Here are some examples:

- distance: $r^* = r/\sigma$
- potential energy: $U^* = U/\epsilon$
- temperature: $T^* = k_B T/\epsilon$
- time: $t^* = t \sqrt{\epsilon/(m\sigma^2)}$
- pressure: $P^* = P\sigma^3/\epsilon$
- density: $\rho^* = \rho\sigma^3$

One very popular choice for the simulated atoms is Argon because it is an inert gas and the atoms behave approximately like hard spheres which attract each other with weak van der Waals forces, which justifies the use of the Lennard-Jones potential. Argon has a mass of $m = 6.69 \times 10^{-26}$ kg, $\sigma = 3.4 \times 10^{-10}$ m and $\varepsilon = 1.65 \times 10^{-21}$ J.

With the above introduced reduced units, the Lennard-Jones potential can be written as

$$U(r^*) = 4 [r^{*-12} - r^{*-6}] . \quad (18)$$

Since the reduced units will be used throughout the rest of this thesis, I will drop the asterisk henceforth.

From the Lennard-Jones potential the corresponding force can be calculated by taking the derivative with respect to the direction of interest:

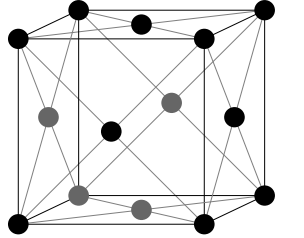
$$\begin{aligned} F_x &= -\frac{\partial}{\partial x} U(r) \\ &= -\frac{\partial}{\partial x} 4 [r^{-12} - r^{-6}] \\ &= -4 [(-12)r^{-13} - (-6)r^{-7}] \frac{\partial r}{\partial x} \\ &= 48 [r^{-13} - 0.5 r^{-7}] \frac{x}{r} \\ &= 48 [r^{-14} - 0.5 r^{-8}] x \end{aligned} \quad (19)$$

The force in the y and z direction can be calculated analogously.

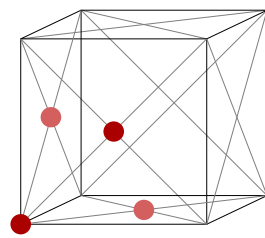
As can be seen in Fig. 5, the potential is very close to 0 at about $r/\sigma = 2.5$. This means that any contribution of the potential energy after this point is vanishingly small. To save computing time it is common practice to cut off the potential at a certain point and not to calculate the contribution for distances beyond that. The cut-off distance for this thesis was set to $r = 2.5\sigma$.

The initial configuration of the particles is a face centered cubic (FCC) lattice. A schematic of the FCC lattice is depicted in Fig. 6a. With the choice of FCC as initial configuration, there are optimal numbers for the numbers of the particles in the system. Since one FCC cell shares its atoms with its next neighbours, the number of atom per unit cell is $4 - 1/8$ of a particle on eight corners and $1/2$ of a particle on six faces. The whole system of atoms is then created by repeating this cell structure. One convenient way is to arrange the unit cells in a cubic system, so if there are M FCC unit cells on one edge, the whole system consists of M^3 cells. Since there are 4 particles per cell, there are ideal or so called *magic numbers* for atoms for which this setup works perfectly: $N = 4M^3 = 4, 32, 108, 256, 500, 864, \dots$

There are several ways to achieve this initial configuration and the one used in



(a) Schematic figure of a face-centered cubic (FCC) lattice.



(b) Setup for successively building a FCC lattice.

this thesis [18] was to create a kind of unit cell consisting of four atoms, as shown in Fig. 6b, which can be described by a set of points

$$\begin{aligned} p_1 &= \{0, 0, 0\} \\ p_2 &= \{0.5 a, 0.5 a, 0\} \\ p_3 &= \{0.5 a, 0, 0.5 a\} \\ p_4 &= \{0, 0.5 a, 0.5 a\} \end{aligned}$$

From the particle number N and the number of FCC unit cells per edge M the *lattice constant* a can be calculated

$$a = \frac{L}{M} \quad (20)$$

where L is the side length of the cube that represents the nano particle and it is calculated via the density of the system

$$L = \sqrt[3]{\frac{N}{\rho}} \quad (21)$$

With the lattice constant and the 4 points of the FCC cell, all the particles can be put into place.

3.4 The Laser Beam - Energy Influx

The nano particle is trapped in the laser beam. While the motion of the center of mass is localized, the individual atoms that make up the glass sphere absorb the energy from the laser which increases their velocity.

To simulate this kind of behaviour, thermostat algorithms [19] such as the Nosé-Hoover [20, 21] or the Andersen [22] algorithms are often used in simulation to change the temperature of the system in a controllable way.

The problem with these kind of algorithms is that a target temperature has to be

fixed which will be reached at some point. In order to simulate the influx of energy from the laser it would be better to have an algorithm that supplies the system with a certain amount of energy continuously. Fortunately, such an algorithm exists.

The algorithm is called Heat Exchange Algorithm (HEX) [23]. Its intended purpose is the use in non-equilibrium molecular dynamics (NEMD) to study transport phenomena and determine transport coefficients. The algorithm works by introducing two regions in the system, one serving as a heat source and the other as a heat sink. A specific amount of heat is then exchanged between those two reservoirs. As it turns out however, this algorithm introduces an energy shift for longer simulation times. This led Wirnsberger et al. [24] to revisit the algorithm and identify the cause of this energy drift, to create a more suitable algorithm, which they called eHEX.

As in the HEX algorithm, regions are introduced to the system which act either as heat sinks or heat sources. These are labelled with Γ_k , where $k > 0$, and have corresponding amount of exchanged heat ΔQ_{Γ_k} . If ΔQ_{Γ_k} is negative, heat is subtracted from the system and vice versa. Regions that neither act as heat source or heat sink are labelled with Γ_0 , which are also called Hamiltonian regions (see Fig. 7). The centers of mass of the particles in simulation box, denoted by Ω , and the regions Γ_k are assumed to be moving with velocities v_Ω and v_{Γ_k} respectively.

The change of the energy in a region Γ_k is achieved by rescaling the velocities by a factor ξ_k and shifted by the velocity of the corresponding region:

$$\mathbf{v}_i \rightarrow \bar{\mathbf{v}}_i = \xi_k \mathbf{v}_i + (1 - \xi_k) \mathbf{v}_{\Gamma_k} \quad (22)$$

The bar over a quantity denotes the value after the exchange of heat.

The factor ξ_k is given by

$$\xi_k = \sqrt{1 + \frac{\Delta Q_{\Gamma_k}}{\mathcal{K}_{\Gamma_k}}} \quad (23)$$

where ΔQ_{Γ_k} is the exchanged heat in the region Γ_k and \mathcal{K}_{Γ_k} is the non-translational kinetic energy of the region Γ_k and is given by

$$\mathcal{K}_{\Gamma_k} = \sum_{i \in \gamma_k} \frac{m_i v_i^2}{2} - \frac{m_{\Gamma_k} v_{\Gamma_k}^2}{2} \quad (24)$$

The sum is taken over all indices in γ_k which is the set of indices of particles in the region Γ_k .

For the final version of the eHEX algorithm there are three more quantities needed. The first one is the heat flux per time step, denoted by \mathcal{F}_{Γ_k} :

$$\mathcal{F}_{\Gamma_k} = \frac{\Delta Q_{\Gamma_k}}{\Delta t} \quad (25)$$

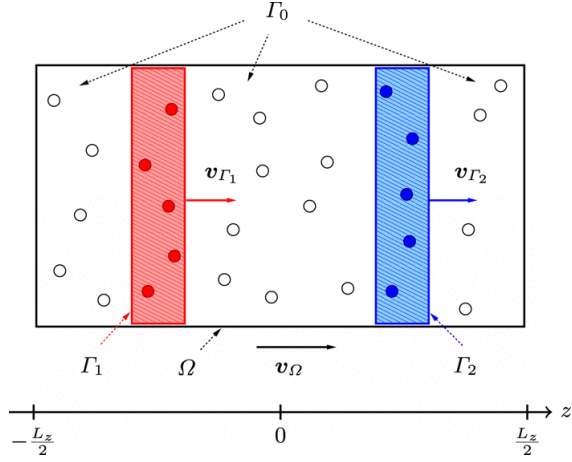


Figure 7: Setup for the use of the HEX and eHEX algorithms. The simulation box Ω , which is moving with a velocity of v_Ω , contains a heat source (red), Γ_1 , which is moving with velocity v_{Γ_1} and a heat sink (blue), Γ_2 , which is moving with velocity v_{Γ_2} . The regions that are neither heat sources or heat sinks are denoted by Γ_0 .

The second one is the thermostating force $\boldsymbol{\eta}_i$, which is defined as

$$\boldsymbol{\eta}_i = \begin{cases} m_i \frac{\mathcal{F}_{\Gamma_{k(\mathbf{r}_i)}}}{2\mathcal{K}_{\Gamma_{k(\mathbf{r}_i)}}} (\mathbf{v}_i - \mathbf{v}_{\Gamma_{k(\mathbf{r}_i)}}) & \text{if } k(\mathbf{r}_i) > 0 \\ 0 & \text{otherwise} \end{cases} \quad (26)$$

where $k(\mathbf{r}_i)$ is the index of the region in which particle i located, i.e. $k(\mathbf{r}_i) = 0$ means that the particle is in a Hamiltonian region and $k(\mathbf{r}_i) > 0$ denotes the heat sinks and sources.

The last quantity is the one that corrects the long term energy drift of the HEX algorithm, denoted by $\mathcal{E}r_{i,\alpha}$. The analysis and derivation of this term is given in [24].

$$\begin{aligned} \mathcal{E}r_{i,\alpha} = & \frac{\eta_{i,\alpha}}{m_i \mathcal{K}_{\Gamma_{k(\mathbf{r}_i)}}} \left[\frac{\mathcal{F}_{\Gamma_{k(\mathbf{r}_i)}}}{48} + \frac{1}{6} \sum_{j \in \gamma_{k(\mathbf{r}_i)}} \mathbf{f}_j \cdot (\mathbf{v}_j - \mathbf{v}_{\Gamma_{k(\mathbf{r}_i)}}) \right] \\ & - \frac{\mathcal{F}_{\Gamma_{k(\mathbf{r}_i)}}}{12\mathcal{K}_{\Gamma_{k(\mathbf{r}_i)}}} \left[\frac{f_{i,\alpha}}{m_i} - \frac{1}{m_{\Gamma_{k(\mathbf{r}_i)}}} \sum_{j \in \gamma_{k(\mathbf{r}_i)}} f_{j,\alpha} \right] \end{aligned} \quad (27)$$

The \mathbf{f} in the above equation denotes the force corresponding to the chosen inter-molecular potential $U(\mathbf{r})$,

$$\mathbf{f} = -\nabla_{\mathbf{r}_i} U(\mathbf{r}_i) \quad (28)$$

With all the necessary quantities established, the updating sequence of the eHEX algorithm can be written down:

$$\bar{\mathbf{v}}_i^n = \xi_{k(\mathbf{r}_i)}^n \mathbf{v}_i^n + (1 - \xi_{k(\mathbf{r}_i)}^n) \mathbf{v}_{\Gamma_{k(\mathbf{r}_i)}}^n \quad (29a)$$

$$\bar{\mathbf{v}}_i^{n+\frac{1}{2}} = \bar{\mathbf{v}}_i^n + \frac{\Delta t}{2m_i} \mathbf{f}_i^n \quad (29b)$$

$$\bar{\mathbf{r}}_i^{n+1} = \mathbf{r}_i^n + \Delta t \bar{\mathbf{v}}_i^{n+\frac{1}{2}} \quad (29c)$$

$$\mathbf{f}_i^{n+1} = -\nabla_{\mathbf{r}_i} U(\mathbf{r})|_{\mathbf{r}=\bar{\mathbf{r}}^{n+1}} \quad (29d)$$

$$\bar{\mathbf{v}}_i^{n+1} = \bar{\mathbf{v}}_i^{n+\frac{1}{2}} + \frac{\Delta t}{2m_i} \mathbf{f}_i^{n+1} \quad (29e)$$

$$\mathbf{v}_i^{n+1} = \bar{\xi}_{k(\bar{\mathbf{r}}_i)}^{n+1} \bar{\mathbf{v}}_i^{n+1} + (1 - \bar{\xi}_{k(\bar{\mathbf{r}}_i)}^{n+1}) \bar{\mathbf{v}}_{\Gamma_{k(\bar{\mathbf{r}}_i)}}^{n+1} \quad (29f)$$

$$\mathbf{r}_i^{n+1} = \bar{\mathbf{r}}^{n+1} - \Delta t^3 \mathcal{E} \bar{\mathbf{r}}_i^{n+1} \quad (29g)$$

This algorithm can be adapted for the problem of the levitating nano sphere in the laser beam by adjusting the setup and some of the parameters.

Firstly, the setup of the heat sinks and sources has to be changed. Since there is only energy pumped into the system from the outside, the region acting as a heat sink vanishes and the region acting as a heat source spans over the whole simulation box. This means that, using the notation of Fig. 7, $\Omega = \Gamma_1$. Furthermore, neither the center of mass of the particles the simulation box nor the heat source are moving, i.e. $\mathbf{v}_\Omega = \mathbf{v}_{\Gamma_1} = 0$. This affects the non-translational kinetic energy term \mathcal{K}_{Γ_1} , the thermostatting force $\boldsymbol{\eta}$ and the correction term $\mathcal{E}\mathbf{r}$. Since there is only one region acting as a heat source, the terms ΔQ , \mathcal{K} and \mathcal{F} don't need an index. The summation index in (24) and (27) can be changed to the number of particles in the system, N , since all the particles are within the heat exchanging region. The masses are set to 1, i.e. $m_i = 1$ with the chosen reduced units and with this the total mass of the region (in the term $1/m_{\Gamma_{k(\mathbf{r}_i)}}$ in (27)) is equal to the number of particles in the system. With these changes, the quantities can be written down

as:

$$\mathcal{K} = \sum_N \frac{v_i^2}{2} \quad (30)$$

$$\xi = \sqrt{1 + \frac{\Delta Q}{\mathcal{K}}} \quad (31)$$

$$\mathcal{F} = \frac{\Delta Q}{\Delta t} \quad (32)$$

$$\boldsymbol{\eta}_i = \frac{\mathcal{F}}{2\mathcal{K}} \mathbf{v}_i \quad (33)$$

$$\begin{aligned} \mathcal{E}r_{i,\alpha} &= \frac{\eta_{i,\alpha}}{\mathcal{K}} \left[\frac{\mathcal{F}}{48} + \frac{1}{6} \sum_N \mathbf{f}_j \cdot \mathbf{v}_j \right] \\ &- \frac{\mathcal{F}}{12\mathcal{K}} \left[f_{i,\alpha} - \frac{1}{N} \sum_N f_{j,\alpha} \right] \end{aligned} \quad (34)$$

This means that the laser is modeled to be pumping energy into the system, which increases the velocities of the particles in the system over time, while the center of mass motion is not affected by this.

3.5 The Laser Beam - Trapping

As mentioned above, the glass particle is trapped in the laser beam and the position of the particle is localized. This behaviour has to be modeled as well.

The approximation of the original paper [9], where the movements in the three spatial directions are decoupled will be used in the model as well. As to the model of the trapping force itself, the most straightforward approach is to use a harmonic oscillator potential. The force and the corresponding potential can be written as

$$\mathbf{F} = -k [\mathbf{r}_{\text{COM}} - \mathbf{x}_0] \quad (35)$$

$$U = \frac{1}{2} k [\mathbf{r}_{\text{COM}} - \mathbf{x}_0]^2 \quad (36)$$

where \mathbf{x}_0 is the position of minimal potential energy, \mathbf{r}_{COM} is the position of the center of mass and k is the spring constant. To calculate the center of mass positions and velocities, the positions and velocities of all particles have to be summed up and divided by the particle number:

$$\mathbf{r}_{\text{COM}} = \frac{1}{N} \sum_{i=1}^N \mathbf{r}_i \quad (37)$$

To use this in the simulation, the distance of the center of mass to the desired point of minimal potential energy and then the corresponding force is calculated and added to the interaction force of each atom.

3.6 Surrounding Gas - Thermostat

Without any equilibrating mechanism the setup described by now would lead to the system heating up indefinitely, which is not desirable. Furthermore, the goal is to recreate the experiment as close as possible. Since the nano particle is trapped in a laser beam within a vacuum chamber, the surrounding gas has to be modeled as well. In the next step we will introduce the surrounding gas of the gas chamber that will absorb some of the energy in the system, leading to the final state.

Generally, pressure is introduced to the system by surrounding the object of interest (in this case the glass nano sphere) with a thermostatted pressure medium. There are two main requirements for the choice of such a pressure medium: the exerted pressure must be hydrostatic and the computation of the interaction between the pressure medium and the object of interest must not take up a lot of resources.

The model used in this thesis was developed by Grünwald and Dellago [25] and uses an ideal gas of non-interacting particles as thermostatted pressure medium. The particles of this pressure medium flow into the simulation from an outside volume, whose geometry is based on the form of the object of interest (this will be referred to as the minimal volume of cells) and leave the simulation box if their position reaches the boundary of this minimal volume of cells. The minimal volume of cells is based on cell lists used in the simulation. Cell lists are a method of saving computing time by dividing the simulation box in cells with a side length equal to or greater than the cutoff radius r_C . The particles are then sorted into these cells and the interaction between the particles is only calculated for other particles within the same and neighbouring cells. For the minimum volume of cells used in the thermostat algorithm all cells filled with particles and one additional cell for the interaction partners is used.

This algorithm is a very good approximation of the situation in the experiment. There the gas particles only interact with the nano particle in the laser trap and not with each other. After this interaction the gas particles emerge with a slightly higher temperature and leave the vicinity of the nano particle. Moreover, the algorithm uses an ideal gas as a pressure medium, which allows us to simulate the dynamics of the interaction that is happening in the experiment.

The gas particles interact with the object via a soft-sphere potential of the

form

$$U(r) = \varepsilon \left(\frac{\sigma}{r} \right)^{12} \quad (38)$$

where ε is the interaction strength, σ is the interaction range and r is the distance between the gas particle and the interacting particle. The gas particles do not interact with one another in this model.

In order to increase the efficiency of the computing process, σ should be chosen carefully. For larger σ , the number of interaction partners increases, which increases the number of force calculations which are a very time consuming part. For smaller σ the possibility for gas particles reaching the inside of the nano particle increases, which is not desirable. So σ should be chosen small enough to keep the force calculations at a minimum and large enough for the particle to stay on the outside of the crystal. In the computer simulations performed for this thesis, the interaction length is chosen to be $\sigma = 1$ with a cut-off radius of $r_c = 2.5$.

The algorithm can be performed by following these steps:

1. Randomly draw the number of particles that are created on a single side of the minimal volume of cells, N_{fac} , from a Poisson distribution with mean value

$$\langle N_{\text{fac}} \rangle = \Delta t L^2 P \sqrt{\frac{1}{2\pi m k_B T}} \quad (39)$$

where Δt is the time step of the simulation, L is the side length of the cell in which the particle is created, P is the desired pressure, m is the mass of the gas particle, k_B is the Boltzmann constant (which will be set to 1 in reduced units) and T is the desired temperature. This chosen number of particles is then uniformly distributed over the face of the cell on which they are created. The velocities of the created particles are drawn from two different random number distributions. The component of the particle velocity perpendicular to the surface is drawn from a Rayleigh distribution of the form

$$p(v_i) = \frac{m}{k_B T} v_i e^{-\frac{mv_i^2}{2k_B T}} \quad (40)$$

The other components of the particles' velocity are drawn from a Maxwell-Boltzmann distribution.

2. Perform the first step of the velocity Verlet algorithm to propagate the particle positions by one time step.
3. Check if any gas particles have left the minimal volume of cells and remove those which have.

4. Check if the geometry of the crystal and with it the minimal volume of cells has changed. If it has, remove all gas particles in the cells that are no longer needed. Then insert new gas particles to the created cells with a number drawn from a Poisson distribution with mean value

$$\langle N_{\text{ins}} \rangle = \frac{PL^3}{k_B T} \quad (41)$$

If the length of the cell L is chosen to be equal to the cut-off radius r_c , this insertion should only be carried out with a probability of

$$P_{\text{ins}} = e^{-\frac{U}{k_B T}} \quad (42)$$

(where U is the interaction energy between the gas particle and the crystal) because it is possible that the inserted particle is within the interaction range of the crystal.

5. Compute all forces.
6. Perform the second step of the velocity Verlet and propagate the particle velocities by one time step.

This algorithm is formulated in a general fashion, so that a wide range of crystals and geometries can be used. Although the shape of the nano particle changes over the course of the simulation, it is not necessary to change the geometry of the surrounding box. The algorithm will therefore not be carried out using cell-lists and a minimal volume of cells that is changing over the course of the simulation, but rather a fixed setup of the volume surrounding the nano particle.

Since the particle itself is modeled as a cube, a straightforward approach is surrounding it by a bigger cube. The distance between the cube face and the nano particle is chosen to be the side length of the nano particle, so the setup will properly scale for different numbers of particles. The schematic setup for this is depicted in Fig.8.

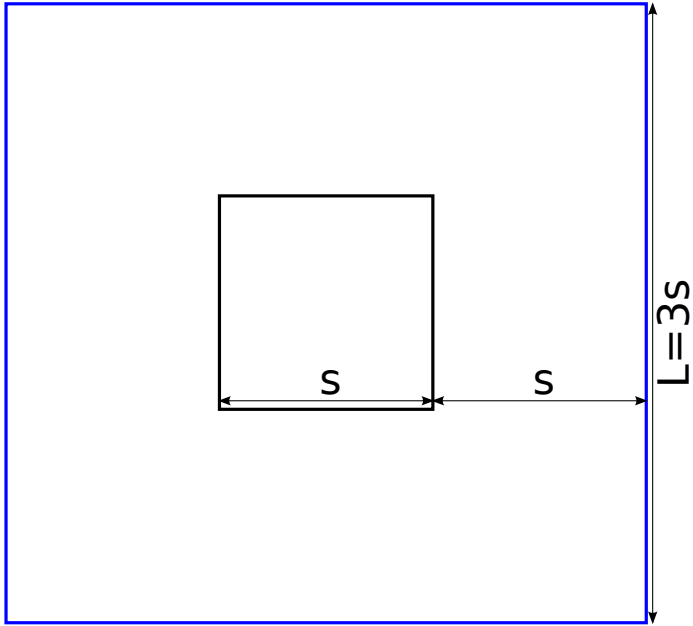


Figure 8: Schematic setup for the barostat. The outer volume (blue) is one side length s away from the nano particle (black) which means that the side length of the face of the surrounding box is $L = 3s$. The gas particles are created along the blue lines of the outer volume. Since the overall geometry of the nano particle does not change, the geometry of the outer volume will be constant throughout the simulation.

4 Results

Since the simulation consists of various parts that have to work together, we first need to check if every part itself works.

4.1 The Crystal

The first element of the simulation is the setup of the FCC lattice on which the particles are placed on. To check if this is done correctly, we can use a visualisation and rendering software such as VMD[26] or OVITO[27]. The rendered image of the nano particle can be seen in Fig. 9. To see that the particles form a FCC lattice a perspective is chosen, where the three layers of the FCC lattice are visible. These layers are generated by stacking the atoms onto the gap between two atoms. In a FCC lattice there are three distinct layers, which means that the atoms of the fourth layer are on the same position as the atoms in the first layer.

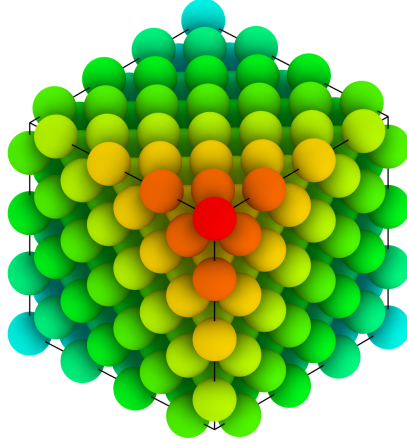


Figure 9: A rendered image of the FCC lattice. The chosen color-coding along the (1,1,1) Miller-index highlights the layers for this perspective. The perspective is chosen to see the layering of the FCC lattice with its 3 layer structure. The black box acts as a reference point to outline the geometry of the system.

4.2 Velocity Verlet

The simulation of the nano particle without the gas is taking place in a NVE ensemble from a thermodynamic point of view. This means that the particle number N , the volume V and the total energy E are constant. The initial velocities of the particles are chosen randomly from a Maxwell-Boltzmann distribution. To ensure that the system behaves the way it is intended to, small adjustments have to be made in the beginning of the simulation of the nano particle.

The first adjustment that needs to be made is making sure that the system is staying in place and not floating away. To do this, the velocity vectors of all the atoms in the system have to be added to get the resulting velocity vector for the whole system. This resulting vector is then divided by the number of particles in the system and the resulting vector is then subtracted from every velocity vector of every atom in the system.

$$\mathbf{v}_{\text{COM}} = \frac{1}{N} \sum_{i=1}^N \mathbf{v}_i \quad (43)$$

$$\mathbf{v}_i^{\text{new}} = \mathbf{v}_i - \mathbf{v}_{\text{COM}} \quad (44)$$

This adjustment only needs to be done just after randomly choosing the velocities, as there is no force present at this point that would cause the nano particle to move.

As mentioned above, the velocities are chosen from a Maxwell-Boltzmann distribution, which means choosing each component from a Gaussian distribution.

However, the positions on the FCC lattice are not very natural and so the atoms equilibrate to a different temperature than desired. If the system should have a specific starting temperature T , the velocities need to be scaled accordingly. This rescaling is done by summing the square of the velocities (this equals calculating the kinetic energy since the masses are set to 1) and rescale them by a factor λ :

$$E = \sum_{i=1}^N \frac{\mathbf{v}_i^2}{2} \quad (45)$$

$$\lambda = \sqrt{\frac{3(N-1)T}{2E}} \quad (46)$$

$$\mathbf{v}_i^{\text{new}} = \lambda \mathbf{v}_i \quad (47)$$

This process has to be done a couple of times, until the system equilibrates to the desired temperature. If we look at the energy values in Fig. 10 we can see the irregularities (jumps) before the system equilibrates to a constant value. This equilibration process divides the simulation in two phases: the equilibration phase and the measurement phase. In the equilibration phase, the system has time to reach a configuration that is (as the name suggests) in an equilibrated state. During this phase, there are usually no measurements (such as energy) performed, since the values from this phase are distorting the mean value of the simulation. That is why the configurations from the equilibration phase are discarded and the measurement phase takes place, where the values do get calculated and are used to determine the mean values.

4.3 eHEX

The next checkpoint is the eHEX algorithm. Since it contains several steps and variables that have to be calculated, this algorithm is very prone to errors. Perhaps the most crucial of those variables in the algorithm is the amount of heat injected into the system, ΔQ . The effect of the value of this variable on the system has therefore to be checked to make sure the system is not overheating.

The investigation of the effects on the system can be done in two ways: comparing the temperature and the energy of the system during the application of the algorithm (similar to the way it's been done with the velocity Verlet) and comparing the effect of different values of ΔQ .

Since the eHEX algorithm injects heat into the system, one would expect the energy and the temperature to rise during the application of the algorithm. In Fig. 11 we can see that exactly this is happening. The graph shows a velocity Verlet phase (that follows an equilibration phase which is not recorded) of constant temperature and energy and an eHEX phase, where the temperature and

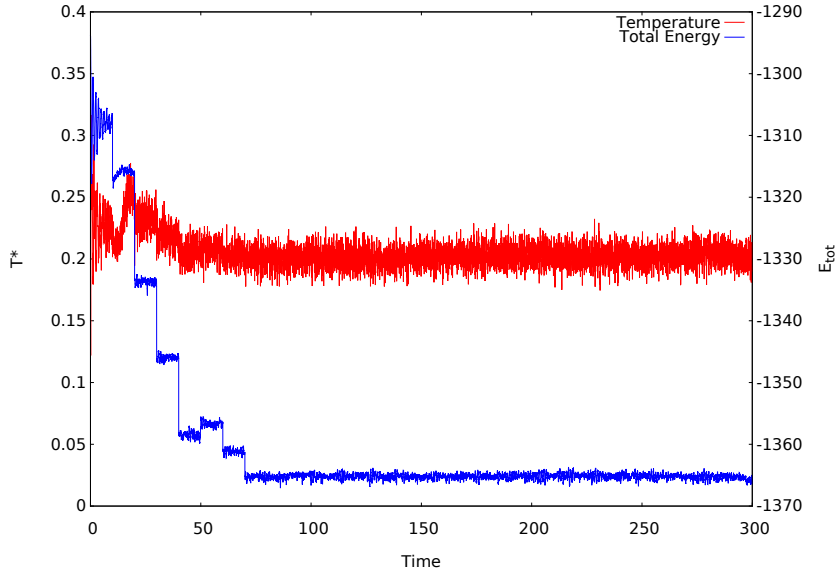


Figure 10: Temperature and energy in the equilibration phase of the velocity Verlet algorithm. The velocity rescaling (see eq. (45)-(47)) is taking place every 1000th step until the 9000th, which can be seen in the energy curve where the jumps are happening. The desired temperature in this case is $T^* = 0.2$, which is reached after about 7000 steps.

the energy are constantly rising. The comparison of different values of ΔQ can be seen in Fig. 12. As the correlation between the temperature and the energy has been shown in Fig. 11, the plotting of the temperature data should suffice.

4.4 Thermostat

The ideal gas thermostat/barostat, as described previously, keeps the system from overheating. The barostat algorithm is applied at the same time as the eHEX algorithm, after the velocity Verlet has equilibrated the system.

The eHEX algorithm is pumping energy into the nano particle while the surrounding gas particles absorb excessive energy. This leads to the development of a new, higher steady temperature of the nano particle, which can be seen in Fig. 13.

4.5 Measurement

Now that the functionality of every individual part has been established, the main question can be tackled: how does the laser intensity influence the center of mass

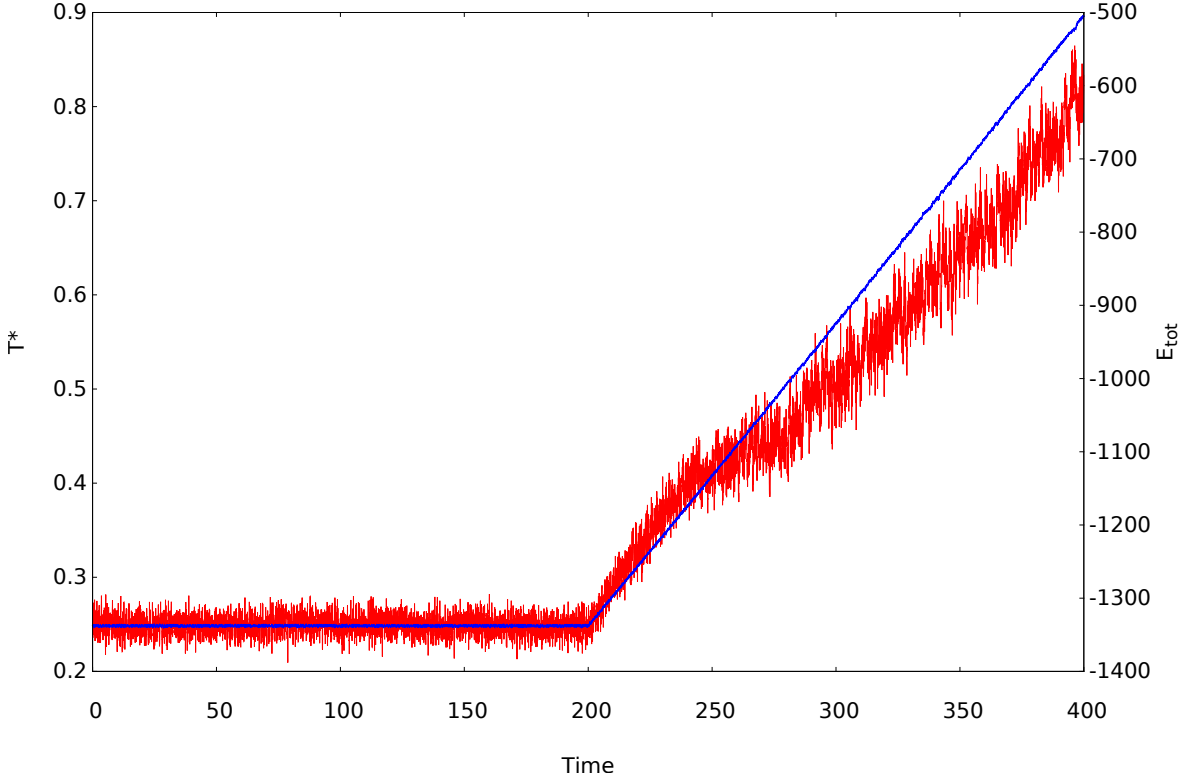


Figure 11: Comparison of temperature (red) and energy (blue) during the application of the eHEX algorithm with $\Delta Q = 0.04$ (in reduced units). The first 20000 timesteps, the energy and temperature are constant during the application of the velocity Verlet algorithm and start to rise, once the eHEX algorithm takes over. The values for the temperature can be seen on the ordinate on the left hand side and the values for the energy on the right hand side.

motion of the nano particle? And which influence does the surrounding gas exert? In order to investigate the origin of the motion of the center of mass, we first need to check whether the eHEX algorithm itself has any influence on the center of mass motion. This is done by applying the algorithm without the thermostat and calculating the center of mass velocity. This turns out to be the case, i.e. the center of mass motion stands still.

To check the integrity of the algorithm, a simple case needs to be tested. Such a simple case is $\Delta Q = 0$, i.e. no energy being pumped into the system. The expected outcome of this case is a thermal equilibration between the incoming gas particles, the outgoing gas particles and the center of mass motion of the nano particle with the incoming gas temperature being the reference value. The measurement yields

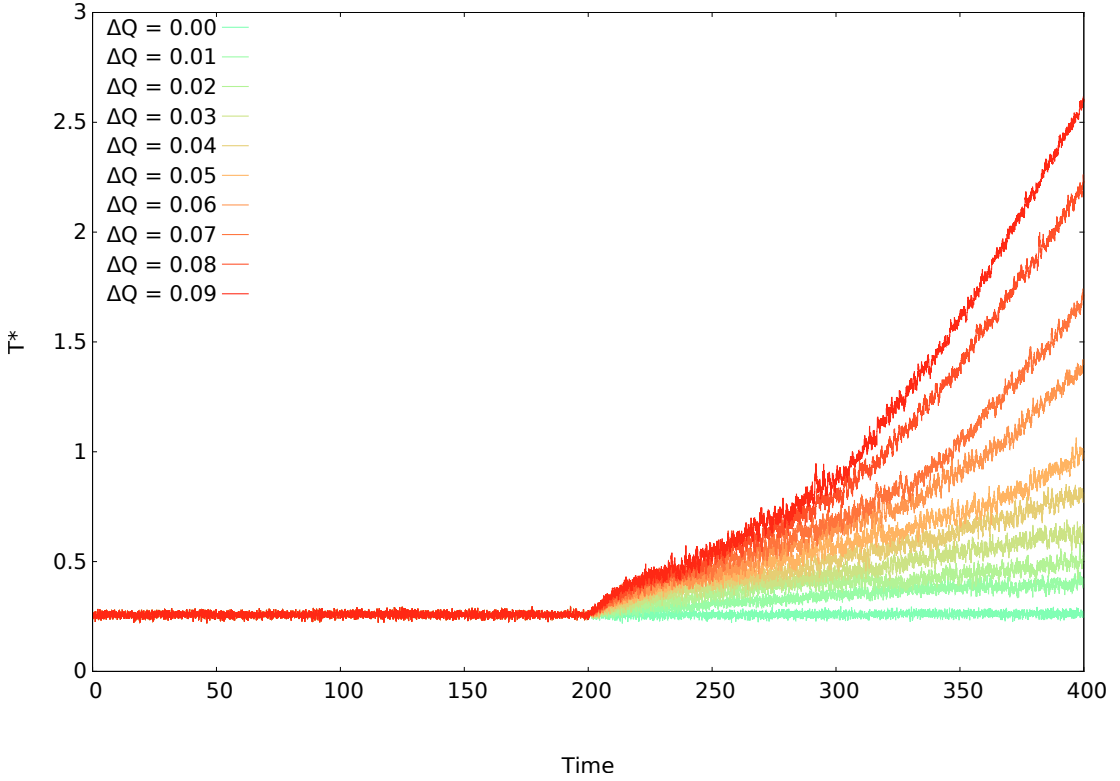


Figure 12: Comparison of different values for ΔQ , ranging from 0 to 0.09. As the value $\Delta Q = 0$ corresponds to no heat being injected into the system, it is not surprising that the temperature remains constant. The graph shows that an increase in ΔQ leads to an increase in the rate of warming up, which means that for bigger ΔQ , the system is heating up more quickly.

this result and backs up the claim. Furthermore, the internal temperature of the nano particle also equilibrates to the temperature of the surrounding gas. This was checked on a system with pressure $P = 0.8$, temperature of the incoming particles $T_{\text{imp}} = 0.05$, internal temperature of the nano particle (set with the velocity verlet) $T_{\text{intern}} = 0.2$ and a system size of $N = 32$ atoms in the nano particle. The resulting temperatures are:

$$\begin{aligned} T_{\text{em}} &= 0.0494 \pm 0.0009 \\ T_{\text{COM}} &= 0.051 \pm 0.108 \\ T_{\text{int}} &= 0.048 \pm 0.007 \end{aligned}$$

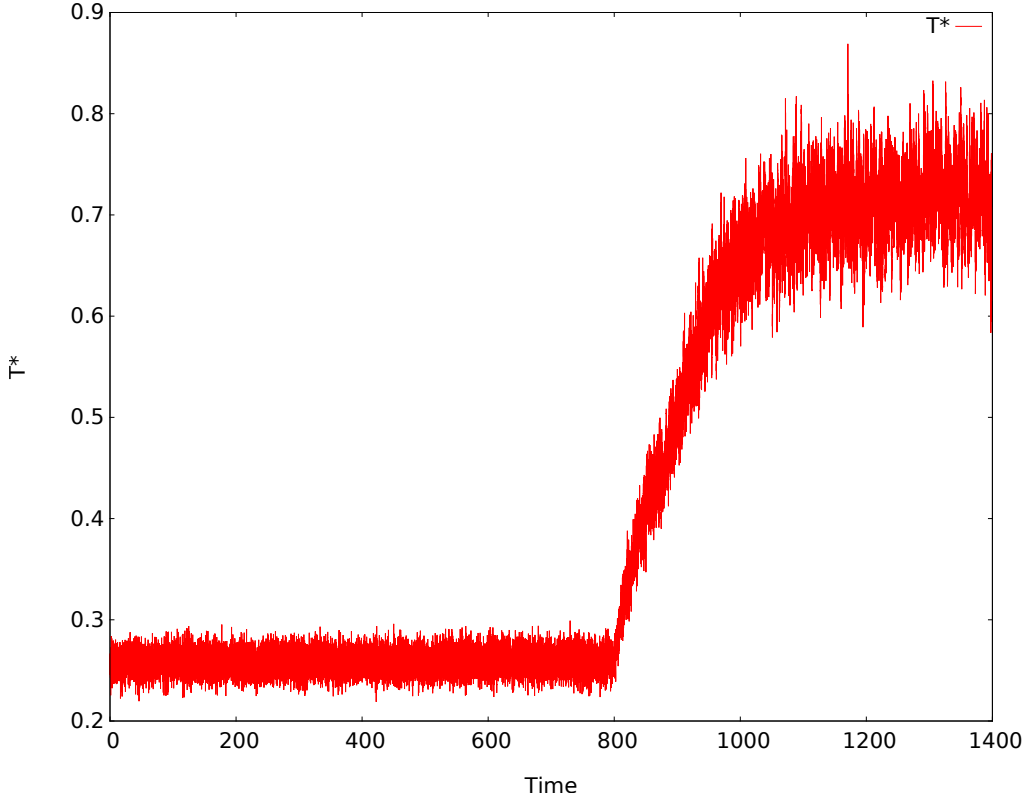


Figure 13: Temperature of the system during the application of the eHEX and the barostat algorithm. During the first 20000 steps the system is in equilibrium while the velocity Verlet algorithm is applied. After that, the eHEX and the barostat algorithms are turned on. This leads to an increase in temperature until a new steady temperature is reached.

The calculation of the temperature is done by using the following equations:

$$E = \frac{m}{2M} \sum_i \vec{v}_i^2 \quad (48)$$

$$E_{\text{Kin}} = \frac{f}{2} k_B T \quad (49)$$

In the first line, m denotes the mass, which is $m = 0.1$ for the gas particles, $m = 1$ for the atoms in the nano particle and $m = 32$ for the center of mass. M denotes the number of particles that are being summed over, which is $M = 1$ for the center of mass, $M = 32$ for the internal temperature and fluctuates for the outgoing gas particles. The number of the outgoing particles is not constant and depends heavily on the pressure and the temperature of the impinging gas

particles, as can be seen in (39). In the second line, f denotes the number of degrees of freedom of the system, which is $f = 3$ for all three systems. Putting these two equations together, we get an equation for the temperature:

$$k_B T = \frac{m}{3M} \sum_i \vec{v}_i^2 \quad (50)$$

Since this describes an instantaneous value, the mean value of the kinetic energy over the course of the simulation has to be used to get the mean value of the temperature of each subsystem. The instantaneous values compared with the mean values can be seen in Figs. 14, 15 and 16.

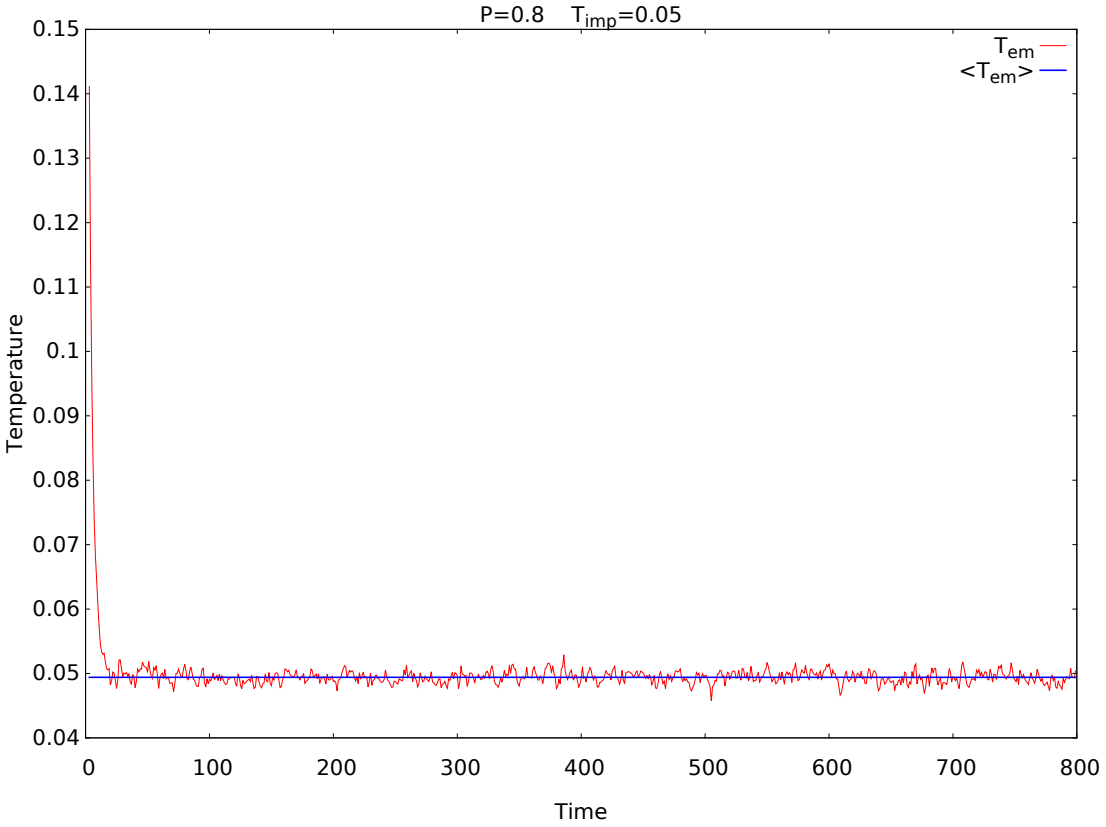


Figure 14: Instantaneous and mean temperature of the outgoing gas particles of the surrounding gas.

With the calculated mean temperature of the center of mass, we can take a look at the distribution of the components of the center of mass velocity. The expected

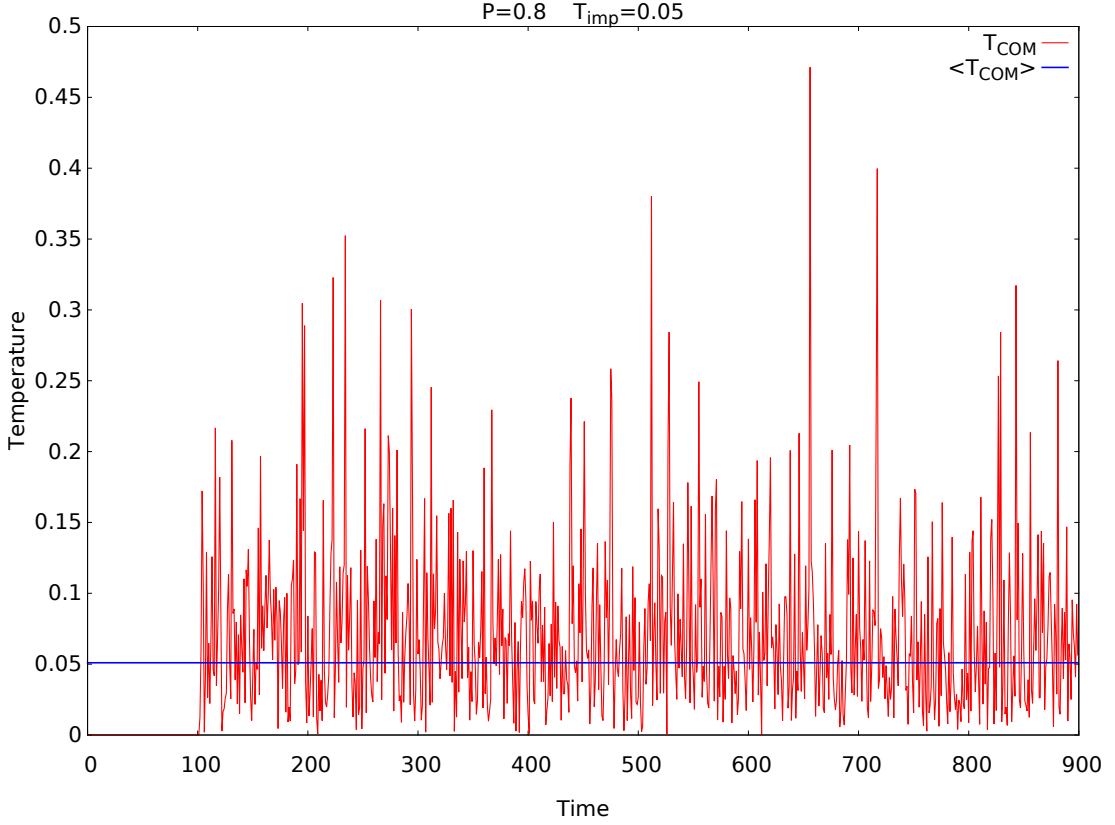


Figure 15: Instantaneous and mean temperature of the center of mass of the nano particle in the laser trap.

distribution is a Gaussian with variance $\sigma^2 = \frac{k_B T}{m}$, i.e.

$$p(v_i) = \sqrt{\frac{m}{2\pi k_B T}} e^{-\frac{x^2 m}{2k_B T}} \quad (51)$$

where i denotes the chosen component of the center of mass velocity vector. A histogram of the x -component of the center of mass velocity with a curve representing eq. (51) can be seen in Fig. 17. Since the y and z axis yield very similar histograms, the x -component has been chosen to represent the velocity components. The graph in Fig. 17 clearly shows, that the velocities indeed follow the Gaussian distribution.

The case of $\Delta Q = 0$ is a good way to start and to check the integrity of the algorithms, but the more interesting cases are the ones where $\Delta Q > 0$. Besides ΔQ , there are two values that determine the dynamics of the system: the pressure P

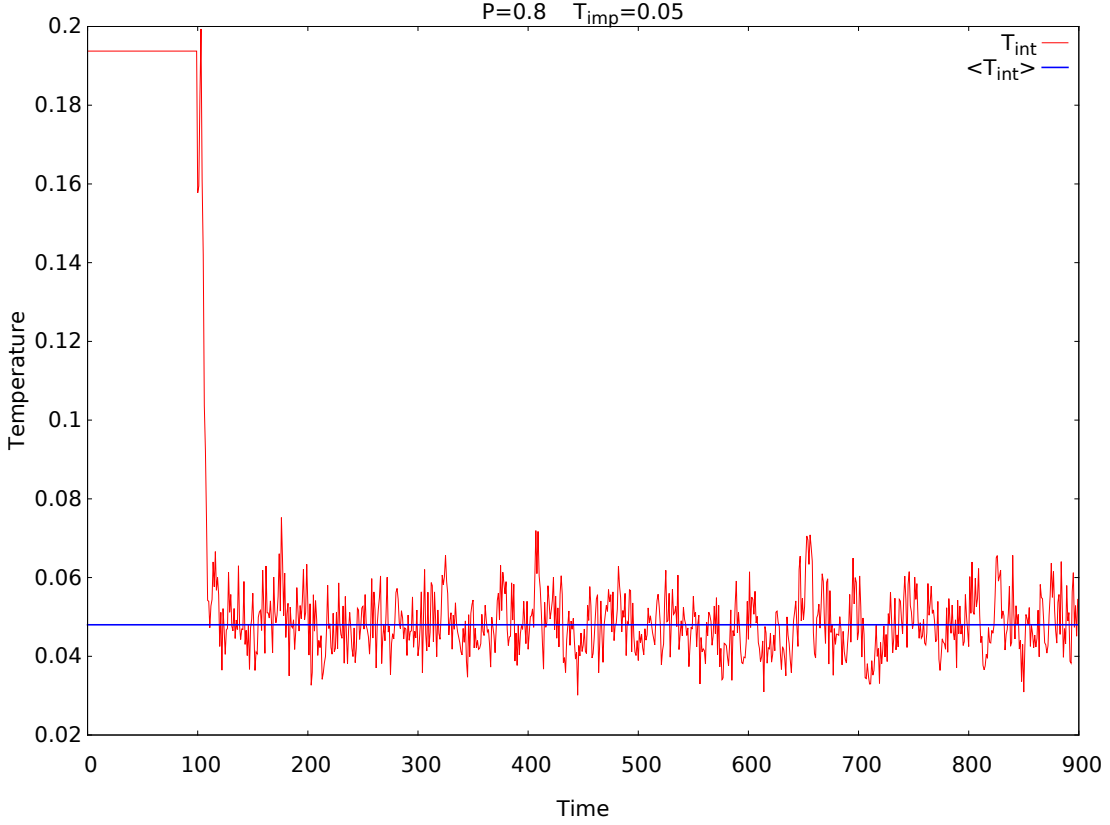


Figure 16: Instantaneous and mean internal temperature of the nano particle in the laser trap.

and the temperature of the impinging gas particles T_{imp} .

Since the surrounding gas acts as a thermostat, the pressure of the impinging gas at a given gas temperature determines the maximum amount of heat that can be pumped into the system without particles of the nano particle leaving the simulation box – the higher the pressure, the more energy can be pumped into the system. The algorithm is applied at two surrounding gas temperatures of $T_{\text{imp}} = 0.05$ and $T_{\text{imp}} = 0.1$, which are one quarter and one half the temperature of the nano particle before applying the eEHX and the thermostat algorithm. The pressure varied from $P = 0.1$ to $P = 1.2$ in steps of $\Delta P = 0.1$ and the heat is generally varied from $\Delta Q = 0$ to $\Delta Q = 0.5$ in steps of 0.05. The term "generally" is used because there are cases where the stepsize has to be decreased or one value for ΔQ is skipped over. The stepsize has to be decreased for low pressures, such as $P = 0.1$ or $P = 0.2$ because there would otherwise not be enough data points.

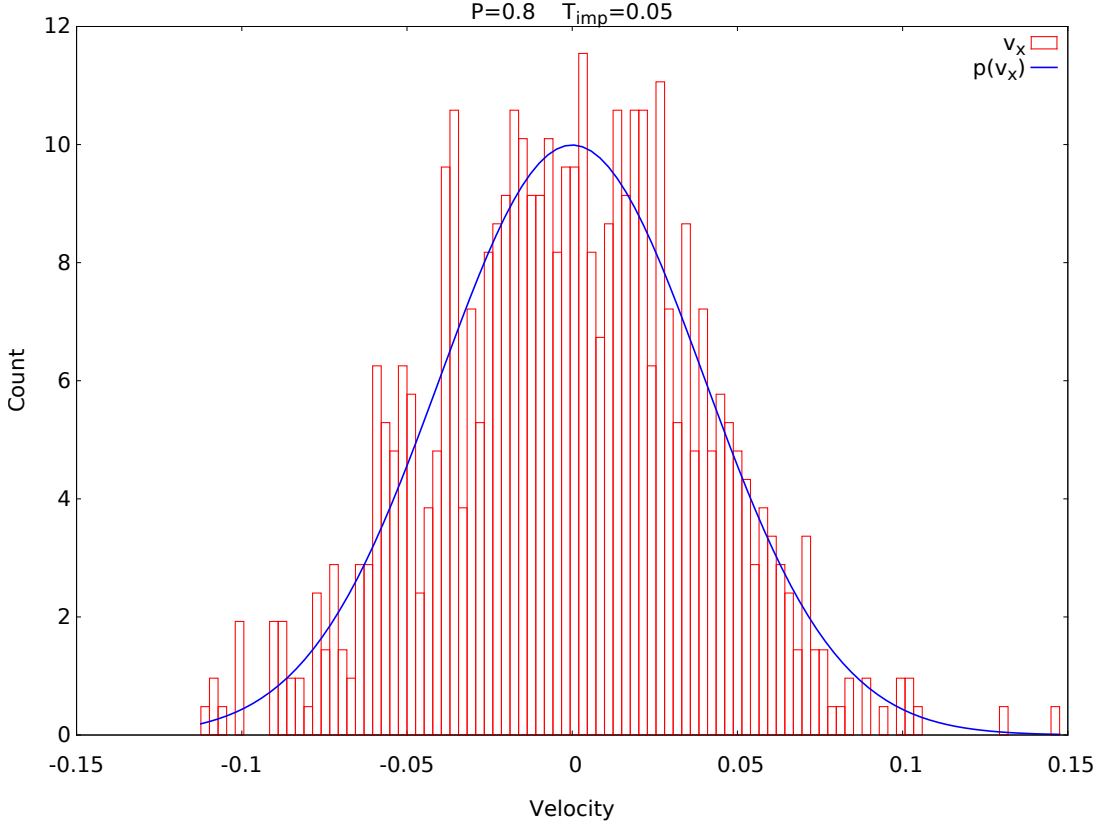


Figure 17: A histogram of the x-component of the center of mass velocities with the expected gaussian distribution.

Some values of ΔQ need to be skipped because it can happen that atoms of the nano particle leave the system due to statistical fluctuations of velocities, which leads to unusable results.

To see the comparison between the different temperatures of the impinging gas temperatures, three values for the pressure are chosen: $P = 0.1$, $P = 0.5$ and $P = 1.0$. The simulation results for the center of mass temperature, the internal temperature and the temperature of the outgoing gas particles are plotted for each of the pressure values and both temperatures, which can be seen in 18. The three columns of the plot correspond to fixed pressure values and different measured quantities, whereas every row corresponds to a fixed measured quantity at different pressures. As previously mentioned, the amount of pressure relates to the number of surrounding particles and thus limits the amount of heat that can be pumped into the system. Therefore, the range of values in the abscissa differs

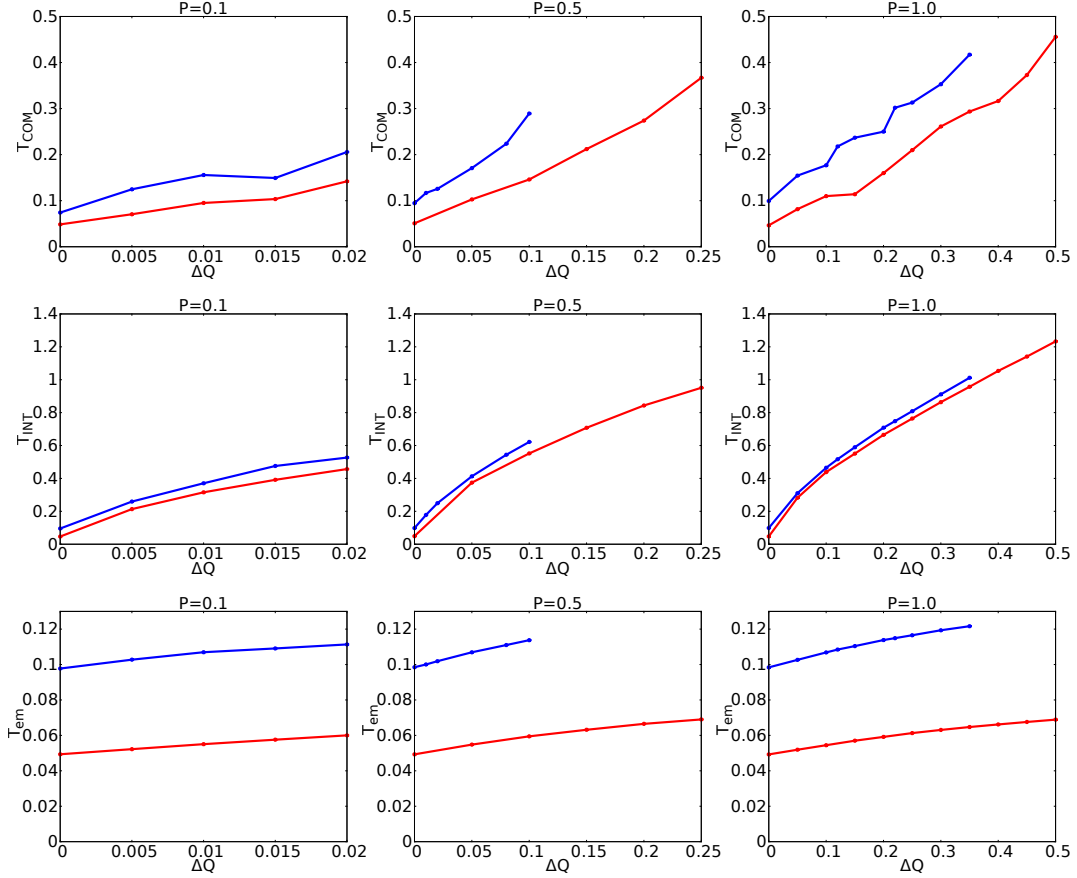


Figure 18: The temperature of the center of mass, the internal temperature and the outgoing temperature of the surrounding gas as functions of heat being pumped into the system, for pressures $P = 0.1$, $P = 0.5$ and $P = 1$ at impinging gas temperatures of $T_{\text{imp}} = 0.05$ (red) and $T_{\text{imp}} = 0.1$ (blue). The three columns each show a fixed pressure value and the rows show fixed measured quantities. As the pressure relates to the maximum amount of heat that can be injected into the system, the ranges on the abscissa in one row is different for every plot.

for different pressures – at $P = 0.1$ the values of ΔQ range from 0 to 0.02 and at $P = 1.0$ from 0 to 0.5.

The first thing that is noticeable, is the increase of the temperature of the center of mass, the internal temperature and the outgoing gas temperature with increasing ΔQ . This makes sense, as the amount of heat that is put into the system is also transferred in the interaction between the nano particle and the surrounding gas. One observation that is not so obvious due to the different ranges of ΔQ values: all temperature values increase faster for low pressures and increase slower for higher pressures. Take the center of mass temperature for $P = 0.1$ and $P = 1$ at $T = 0.05$ (red line) as an example: while it reaches a value of a $T_{\text{com}} = 0.1$ at about $\Delta Q = 0.015$ at $P = 0.1$, it takes a ΔQ of a little under 0.1 to achieve the

same value for $P = 1$. This can be observed for every one of the three quantities. This is to be expected, as the surrounding gas acts as a thermostat.

The development of the different temperatures seem to be depending of the temperature of the surrounding gas as well. The blue curves (which correspond to a surrounding gas temperature of $T = 0.1$) are growing slightly faster than the red curves ($T = 0.05$).

In their paper [12] Millen et al. give a formula for the center of mass temperature:

$$T_{\text{COM}} = \frac{T_{\text{imp}}^{3/2} + \frac{\pi}{8} T_{\text{em}}^{3/2}}{T_{\text{imp}}^{1/2} + \frac{\pi}{8} T_{\text{em}}^{1/2}} \quad (52)$$

This formula together with the measured values of T_{imp} and T_{em} can be used to compare the results. The comparison between the calculated and the measured value can be seen for a representative choice of parameters in Fig. 19. There it becomes obvious, that the measured center of mass temperature rises quicker than the calculated value. This is also the case for different pressures and impinging gas temperatures. The reason for this may be in the difference of the accomodation factor α . In the paper, Millen et al. use an accomodation factor for a sphere with a value of $\alpha = 0.777$, whereas the accomodation factor for the setup in the simulation for the chosen values is around $\alpha = 0.016$. This means that the real and the modeled interaction between the gas particles and the nano particle differ from one another.

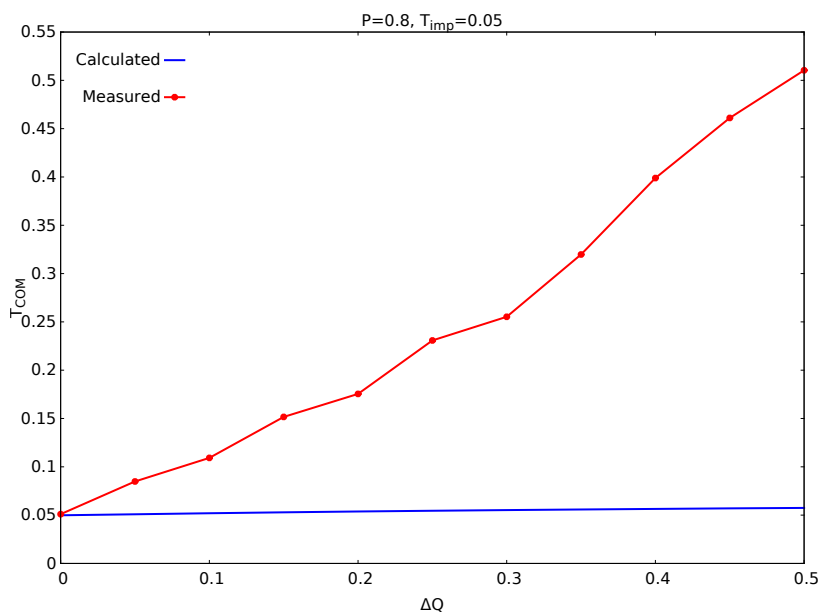


Figure 19: Comparison between the measured (red) and calculated (blue) center of mass temperature according to [12].

5 Conclusion and Further Remarks

In this thesis I have modeled an optical tweezer experiment with methods from the field of computational physics. The experiment was broken down into different sections, that have been modeled separately. With the use of molecular dynamics I simulated the behaviour of a nano particle in a laser trap and investigated the effects of the laser power and temperature of the surrounding gas on the center of mass movement of the nano particle.

The results show, that the center of mass temperature (and thus its movement) does indeed depend on the energy of the laser, as well as on the pressure and temperature of the surrounding gas.

The development of the center of mass temperature shows a curve that seems to have a convex form, whereas the internal temperature shows a more concave behaviour. So while the internal temperature initially grows faster, it could be possible for the center of mass temperature to pass the internal temperature.

There are several ways to explore this subject further. The first idea would be to decrease the pressure even more and investigate the case of very low energies, since this is not easily feasible in an experimental setup. Another idea would be to increase the number of atoms in the nano particle to see if the surface of the particle plays a role in the development of the temperatures. Furthermore, the interaction between the gas particles and the nano particle in the trap could be varied to include an attractive part in the potential. Generally, these simulations could be expanded by running them on faster computers to investigate long term behaviour of the systems and expand the ranges of the different values like pressure or laser energy.

References

- [1] Nicholas Metropolis, Arianna W. Rosenbluth, Marshall N. Rosenbluth, Augusta H. Teller, and Edward Teller. Equation of state calculations by fast computing machines. *The Journal of Chemical Physics*, 21(6):1087–1092, 1953.
- [2] Onofrio M Maragò, Philip H Jones, Pietro G Gucciardi, Giovanni Volpe, and Andrea C Ferrari. Optical trapping and manipulation of nanostructures. *Nature nanotechnology*, 8(11):807–819, 2013.
- [3] Peter Lebedew. Untersuchungen über die druckkräfte des lichtes. *Annalen der Physik*, 311(11):433–458, 1901.
- [4] E. F. Nichols and G. F. Hull. A preliminary communication on the pressure of heat and light radiation. *Phys. Rev. (Series I)*, 13:307–320, Nov 1901.
- [5] A. Ashkin. History of optical trapping and manipulation of small-neutral particle, atoms, and molecules. *IEEE Journal of Selected Topics in Quantum Electronics*, 6(6):841–856, Nov 2000.
- [6] Karel Svoboda and Steven M. Block. Optical trapping of metallic rayleigh particles. *Opt. Lett.*, 19(13):930–932, Jul 1994.
- [7] Shida Tan, Herman A. Lopez, Colin W. Cai, and Yuegang Zhang. Optical trapping of single-walled carbon nanotubes. *Nano Letters*, 4(8):1415–1419, 2004.
- [8] Liselotte Jauffred, Andrew C. Richardson, and Lene B. Oddershede. Three-dimensional optical control of individual quantum dots. *Nano Letters*, 8(10):3376–3380, 2008. PMID: 18767883.
- [9] Jan Gieseler, Romain Quidant, Christoph Dellago, and Lukas Novotny. Dynamic relaxation of a levitated nanoparticle from a non-equilibrium steady state. *Nat Nano*, 9(5):358–364, May 2014.
- [10] Gavin E. Crooks. Entropy production fluctuation theorem and the nonequilibrium work relation for free energy differences. *Phys. Rev. E*, 60:2721–2726, Sep 1999.
- [11] Debra J. Searles and Denis J. Evans. Fluctuation theorem for stochastic systems. *Phys. Rev. E*, 60:159–164, Jul 1999.

- [12] Millen J., Deesawan T., Barker P., and Anders J. Nanoscale temperature measurements using non-equilibrium brownian dynamics of a levitated nanosphere. *Nat Nano*, 9(6):425–429, June 2014.
- [13] Klaus Kroy. Levitating nanoparticles: Non-equilibrium nano-thermometry. *Nat Nano*, 9(6):415–417, June 2014.
- [14] D. Frenkel and B. Smit. *Understanding Molecular Simulation: From Algorithms to Applications*. Computational science series. Elsevier Science, 2001.
- [15] M. P. Allen and D. J. Tildesley. *Computer Simulation of Liquids*. Clarendon Press, New York, NY, USA, 1989.
- [16] Loup Verlet. Computer "experiments" on classical fluids. i. thermodynamical properties of lennard-jones molecules. *Phys. Rev.*, 159:98–103, Jul 1967.
- [17] William C. Swope, Hans C. Andersen, Peter H. Berens, and Kent R. Wilson. A computer simulation method for the calculation of equilibrium constants for the formation of physical clusters of molecules: Application to small water clusters. *The Journal of Chemical Physics*, 76(1):637–649, 1982.
- [18] Idea taken from the Molecular Dynamics part of this lecture: <http://www.physics.buffalo.edu/phy411-506/>.
- [19] Philippe H. Hünenberger. *Thermostat Algorithms for Molecular Dynamics Simulations*, pages 105–149. Springer Berlin Heidelberg, Berlin, Heidelberg, 2005.
- [20] Shuichi Nosé. A unified formulation of the constant temperature molecular dynamics methods. *The Journal of Chemical Physics*, 81(1):511–519, 1984.
- [21] William G. Hoover. Canonical dynamics: Equilibrium phase-space distributions. *Phys. Rev. A*, 31:1695–1697, Mar 1985.
- [22] Hans C. Andersen. Molecular dynamics simulations at constant pressure and/or temperature. *The Journal of Chemical Physics*, 72(4):2384–2393, 1980.
- [23] B. Hafskjold, T. Ikeshoji, and S. Kjelstrup Ratkje. On the molecular mechanism of thermal diffusion in liquids. *Molecular Physics*, 80:1389–1412, December 1993.
- [24] P. Wirnsberger, D. Frenkel, and C. Dellago. An enhanced version of the heat exchange algorithm with excellent energy conservation properties. *The Journal of Chemical Physics*, 143(12), 2015.

- [25] M. Grünwald and C. Dellago. Ideal gas pressure bath: a method for applying hydrostatic pressure in the computer simulation of nanoparticles. *Molecular Physics*, 104(22-24):3709–3715, 2006.
- [26] William Humphrey, Andrew Dalke, and Klaus Schulten. VMD – Visual Molecular Dynamics. *Journal of Molecular Graphics*, 14:33–38, 1996.
- [27] Alexander Stukowski. Visualization and analysis of atomistic simulation data with ovito—the open visualization tool. *Modelling and Simulation in Materials Science and Engineering*, 18(1):015012, 2010.